Aeration of a Free Jet Above a Spillway — **Source link** ↗

Hubert Chanson

Institutions: University of Queensland

Related papers:

- A Study of Air Entrainment and Aeration Devices on a Spillway Model

- Flow downstream of an aerator - aerator spacing

- Ski Jump Hydraulics

- Model Study of Spillway Aerator Device

- A Study of Air Entrainment: Application to Spillway Design = Etude des Phenomenes d'Entrainement d'Air: Application aux Evacuateurs de Crues

Aeration of a free jet above a spillway
Aération d'un jet libre sur un évacuateur de crues

H. CHANSON

Lecturer in Hydraulics/Fluid Mechanics,
Dept. of Civil Engineering, University of Queensland,
St. Lucia, QLD 4072, Australia

SUMMARY

A study of air entrainment above an spillway aerator is presented and discussed with a dimensional analysis. We conclude that similitude of air entrainment processes for spillway aerator is not possible between model and prototype. New informations on the aeration region are presented and an analytical solution of the upper nappe entrainment is developed.

RÉSUMÉ

L'article présente une étude de l'entraînement d'air pour un dispositif d'aération d'écoulements sur un évacuateur de crues, complétée par une étude adimensionnelle. Cette étude conclut que la similitude des processus d'entraînement d'air, pour les aérateurs d'évacuateur de crues, n'est pas possible entre un modèle et un prototype. Cependant de nouveaux résultats sont présentée pour la zone d'aération de l'écoulement et une solution analytique est développée pour l'entraînement à travers la nappe supérieure du jet libre.

1 Introduction

1.1 *Presentation*

At high flow velocities cavitation damage may occur on the spillway surface and leads to a catastrophic failure. With flow velocities greater than 20 to 25 m/s it becomes usual to protect the spillway surface by increasing the compressibility of the fluid near the surface through aeration. The entrained air through the free surface may protect the spillway floor from cavitation damage if the free surface aeration process provides a sufficient air concentration near the bottom [8, 9]. If there is not enough natural free surface aeration (i.e. downstream of a gate), the use of aeration device (called aerator) can provide small quantities of air near the spillway floor which prevent the cavitation damage [12]. Aerators are located on the spillway floor (Fig. 1) and sometimes on the side walls. Vischer et al. [12] detailed the properties of various types of aeration device. Usually a combination of an offset, a ramp and a groove provides the best design.

We propose to study the air entrainment processes of a free jet above a spillway. Firstly a dimensional analysis is presented. Then the aeration region and the processes occurring in this region are detailed.

1.2 *Definition*

The local air concentration is defined as the volume of air per unit volume and this will normally be taken as a time averaged value. Let define the characteristic depth d as:
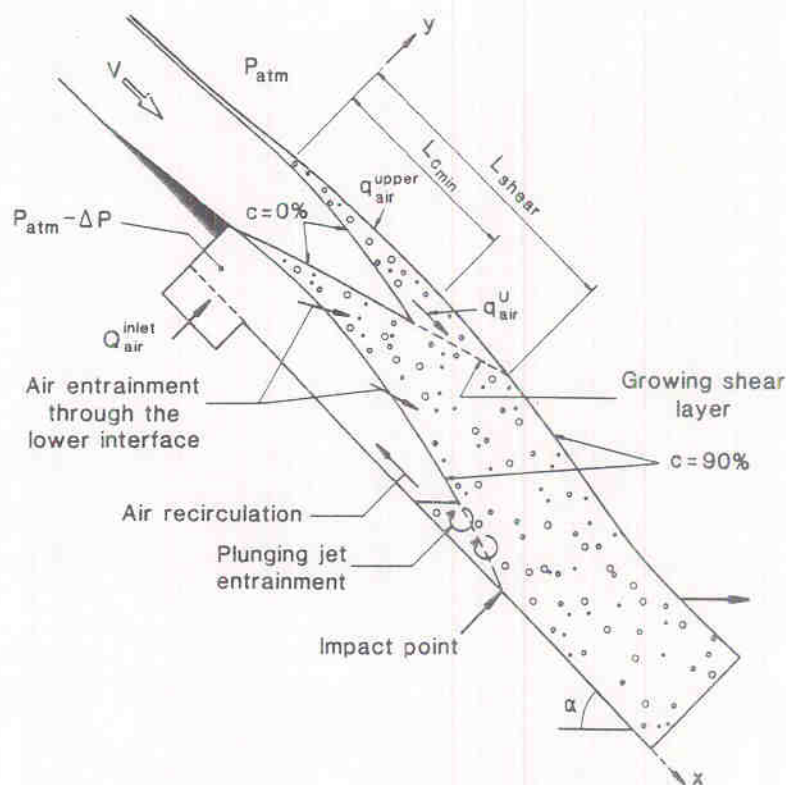

Fig. 1.   Air entrainment above an aeration device.
Entraînement d'air au-dessus d'un système d'aération.

$$d = \int_{0}^{Y_{90}} (1 - C) * dy \tag{1}$$

where y is measured perpendicular to the spillway surface. We also define the characteristic depth of self-aerated flow Y_{90} where the local air concentration is 90%. An average water velocity is:

$$U_w = \frac{q_w}{d} \tag{2}$$

A characteristic water velocity V_{90} is defined as that at Y_{90}. A depth averaged mean air concentration for the flow can be defined from:

$$(1 - C_{mean}) * Y_{90} = d \tag{3}$$

1.3   Experiments

The author performed experiments on a $1:15$ scale model of the Clyde dam spillway (New Zealand) with a slope $\alpha = 52.33°$. The model provided Froude numbers in the range 3 up to 25 with initial average flow velocities from 3 to 14 m/s. The aerator configuration had no ramp and an offset of 30 mm height as that used by Tan [11]. The author performed air concentration and velocity measurements for various Froude numbers at different cross-sections along the spillway model. These experiments were obtained using conductivity probes for air concentration and velocity measurements [1].

2 Air entrainment above a spillway

2.1 *Presentation*

The flow regions above an aerator on steep spillway are defined as the approach flow region, the transition region, the aeration region, the impact point region and the downstream flow region (Fig. 2). The aeration region will be detailed in the next paragraph.

The flow conditions in the approach flow region characterize the initial conditions of the flow above an aerator and some of the surface may be aerated. The transition region coincides with the length of the ramp. The deflector changes the perpendicular pressure field and increases the shear stress on the spillway floor.

The impact region extends from the point where the nappe re-attaches to the bottom of the chute to the beginning of the downstream flow region. The flow is highly turbulent and a high energy loss occurs. In the downstream flow region the air concentration and velocity distributions gradually change and tend to equilibrium profiles far downstream of the aerator [3, 13].
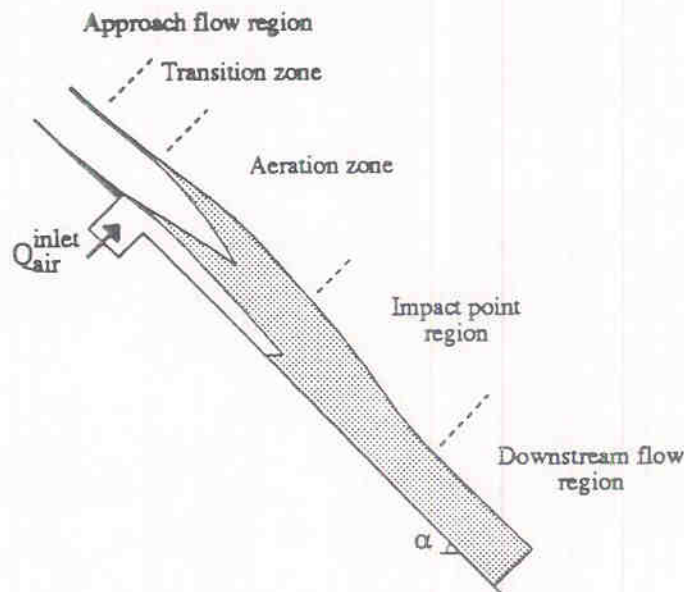

Fig. 2.   Air entrainment regions on a spillway.
Régions d'entraînement d'air sur un évacuateur de crues.

2.2 *Dimensionless parameters*

The parameters required to design an aerator are the air discharge supplied by the inlets Q_{air}^{inlet}, the air concentration near the floor downstream of the aerator C_b, the pressure difference across the nappe ΔP and the water jet length L_{jet}. The author [1] showed that each of these design parameters is a function of the initial independent parameters:

$$L_{jet}, Q_{air}^{inlet}, \Delta P, C_b = f(\varrho_w, \varrho_{air}, \mu, \sigma, g, \alpha, W, k_s, t_s, L_g, A_d, \phi, L_{ramp}, V, d_0, u') \tag{4}$$

Studies are performed on geometrically similar models and it is convenient to use a slice model. Side effects may appear due to the boundary layers on the side walls. However if these boundary effects are assumed small the problem becomes a two-dimensional study. The nappe subpressure is usually controlled by valves on the air inlet systems and this enables the underpressure to be treated as an independent parameter. In addition the density ratio is almost independent and for a

given aerator configuration (a, W, k_s, t_s, L_g, A_d, ϕ, L_{ramp} fixed) the equation (4) is rewritten in terms of dimensionless parameters:

$$\frac{L_{\text{jet}}}{d_0}, \beta^{\text{inlet}}, C_b = f(Re, Fr, We, Tu, P_N) \tag{5}$$

2.3 Air entrainment similitude

The study of air entrainment is complex because of the interaction between different air entrainment processes : air entrainment through the upper and lower free surfaces called nappe entrainment, plunging jet entrainment at the intersection of the jet with the rollers and air recirculation in the cavity below the jet (Fig. 1).

For a vertical plunging jet a dimentional analysis yields [13]: $\beta = f(Fr, P_N)$. At the free surfaces air is entrained by high intensity turbulent eddies close to the interface and Ervine and Falvey [6] suggest that some important processes in turbulent jets in the atmosphere are dependent on the turbulence intensity, the Weber and Reynolds numbers. Each of these air entrainment processes yields a different dimensionless equation and the interaction between these processes must be considered. It is believed that dimensional analysis cannot provide a simple relationship and similitude of air entrainment for spillway aerator is not usually possible between model and prototype.

However simple considerations on the continuity equation for air above an aerator [2] provide the relationship:

$$q_{\text{air}}^{\text{upper}} + \frac{Q_{\text{air}}^{\text{inlet}}}{W} = q_{\text{air}} - q_{\text{air}}^0 \tag{6}$$

where $q_{\text{air}}^{\text{upper}}$ is the net air entrainment through the upper free surface, q_{air}^0 is the initial quantity of air entrained within the flow and q_{air} is the quantity of air entrained within the flow at the end of the free jet (Fig. 1).

The air discharge supplied by the air inlets is usually studied as a function of the subpressure in the cavity ΔP and the flow conditions for a given aerator geometry. This relationship called the air demand of the aerator was detailed by Tan [11], Low [7] and Chanson [4] for the Clyde model. We now propose to detail the nappe entrainment and the upper free surface aeration.

3 The aeration region

3.1 Presentation

When the jet leaves the deflector there is a region with a clear water inner core called the free surface aeration region. If the water jet is long enough the central core of the jet becomes aerated (Figs. 1, 3) and air exchange may occur between the upper and lower part of the jet. This region is called the fully aerated flow region.

3.2 Study of the free-surface aeration region

In the free surface aeration region an analysis of the continuity equation for air [2] shows that the air concentration profiles are fitted by Gaussian curves. If we define the air-water interface of the jet as the iso-air concentration line $C = 90\%$ the air entrainment through that interface may be computed at a distance L from the end of the deflector as:
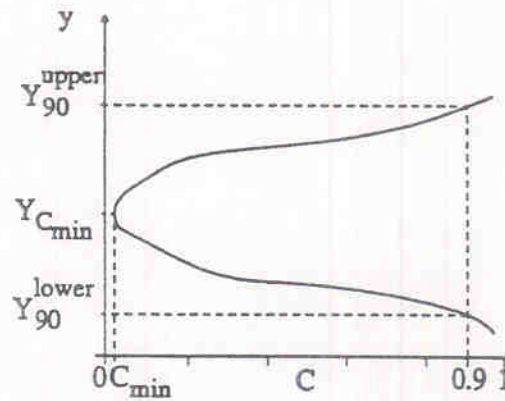
Fig. 3.   Air concentration distribution in the aeration region,
$Fr = 19.2 - d_0 = 0.0351$ m, $P_N = 0.0198 - L/d_0 = 10.1$.

Distribution de la concentration en air dans la zone d'aération.

$$q_{air}^{upper} = \int_0^L \left(D * \frac{dC}{dy} - C * u_r * \cos \theta \right)_{y=Y_{90}} * dx \tag{7}$$

where C is the air concentration, D the diffusivity, u_r the rise bubble velocity and θ the angle between the water jet and the horizontal. The analytical solution of the equation (7) is (appendix 1):

$$\frac{q_{air}^{upper}}{q_w} = K_0 * \left(\frac{L}{d_0} - 2 * \beta^0 * LN \left(1 + \frac{1}{2} * \frac{\tan \psi}{\beta^0} * \frac{L}{d_0} \right) \right) - 0.90 * \frac{L}{d_0} * \frac{u_r}{U_w} * \cos \alpha \tag{8}$$

where

$$K_0 = \frac{1}{\sqrt{2 * \pi}} * e^{-0.5*(1.2817)^2}$$

and ψ is the lateral spread of the jet computed between Y_{90} and Y_{10}. The author's experiments show that for low pressure gradient (Fig. 4a) the angle of the jet spread may be estimated as a first approximation as $\psi^U = 0.75°$ and $\psi^L = 2.5°$ a t the upper and lower interfaces. The Fig. 4b presents the results when the air inlets are sealed $(Q_{air}^{inlet} = 0)$ and the spread angle might be expected to be a function of the pressure gradient.
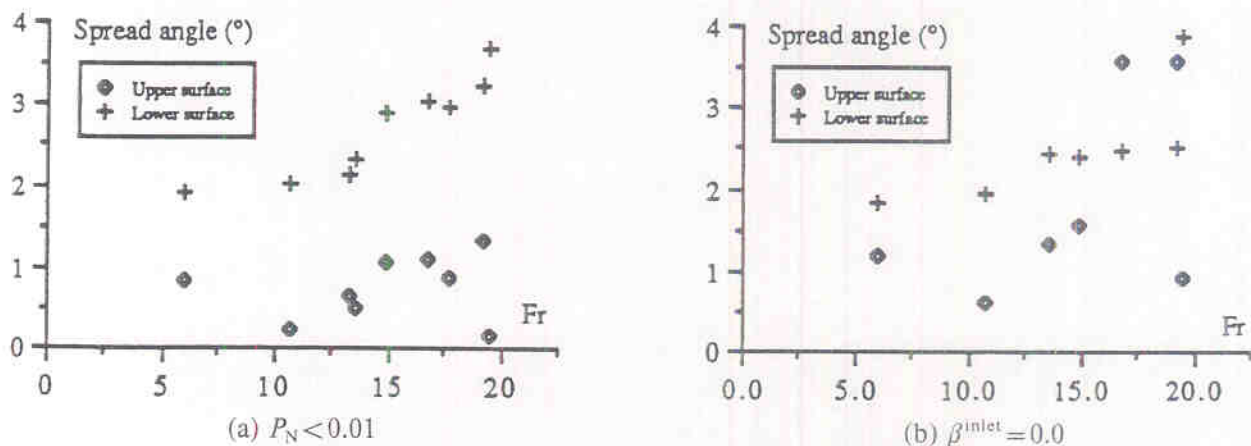

(a) $P_N < 0.01$

(b) $\beta^{inlet} = 0.0$

Fig. 4.   Lateral spread angle computed between Y_{90} and Y_{10}.

Angle d'étalement latéral calculé entre Y_{90} et Y_{10}.

Near the upper interface the flow is very aerated and the author's experiments indicate that bubble diameters of 5–10 mm might be expected. At the end of the deflector jet is submitted to a negative pressure gradient and the rise bubble velocity becomes a fall velocity. An estimate of the bubble velocity may be deduced from Comolet's [5] formulation (Appendix 2):

$$u_r^2 = \left(0.52 * g * d_b + 2.14 * \frac{\sigma}{\varrho_w * d_b}\right) * \left| - P_N * \cos\theta + \frac{\varrho_{air}}{\varrho_w}\right| \tag{9}$$

where d_b is the bubble diameter. In the free surface aeration region the presence of a clear water core prevents air exchange between the upper and lower parts of the jet and the continuity equation for air in the upper flow region becomes (Fig. 1):

$$q_{air}^U = q_{air}^{upper} + q_{air}^0 \tag{10}$$

where q_{air}^U is the quantity of air entrained within the upper region of the flow. On the Fig. 5 the author's data

$$\beta^U = \frac{q_{air}^U}{q_w}$$

are compared with the upper nappe entrainment

$$\frac{q_{air}^{upper} + q_{air}^0}{q_w}$$

computed from the equation (8) with $\psi^U = f(P_N)$ (Fig. 4), $d_b = 5$ mm and $u_r = f(P_N)$ (equation (9)). The results are within the accuracy of the data and this suggests that the assumptions are reasonable and that the equation (8) is a good estimate of the upper nappe entrainment in the free surface aeration region($0 < L < L_{C_{min}}$).
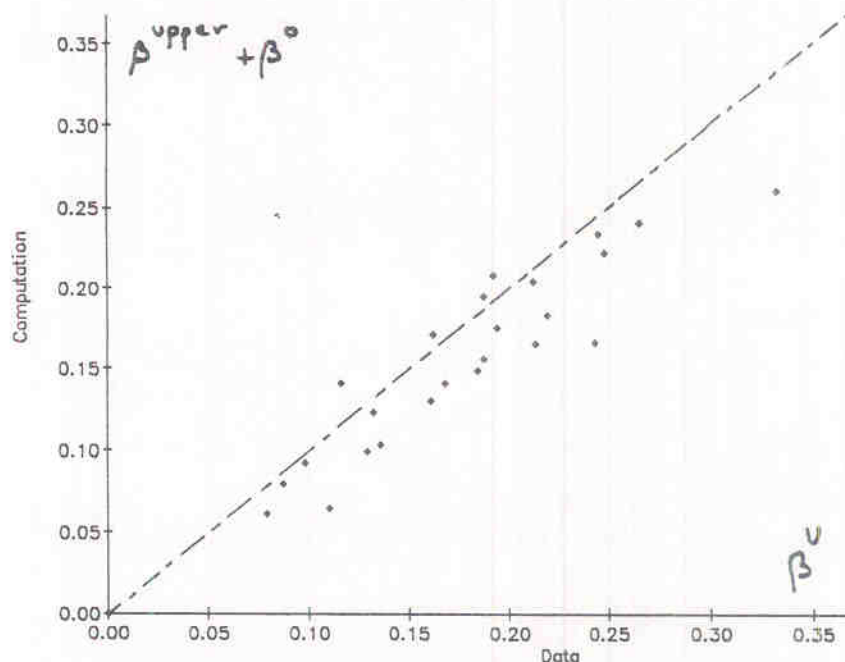

Fig. 5.   Comparison between the quantity of air entrained within the upper region computed as $(q_{air}^0 + q_{air}^{upper})/q_w$ and the author's data β^U for $0 < L < L_{C_{min}}$.

Comparaison entre la quantité d'air entraînée à l'intérieur de la zone supérieure, calculée par $(q_{air}^0 + q_{air}^{upper})/q_w$ et les résultats de l'auteur β^U pour $0 < L < L_{C_{min}}$.

An application is presented on the Fig. 6 where the quantity of air entrained is plotted as a function of the distance L from the end of the deflector. It must be emphasized that these calculations only apply in the free surface aeration and depend critically on the assumed bubble size d_b and the lateral spread angle ψ^U.

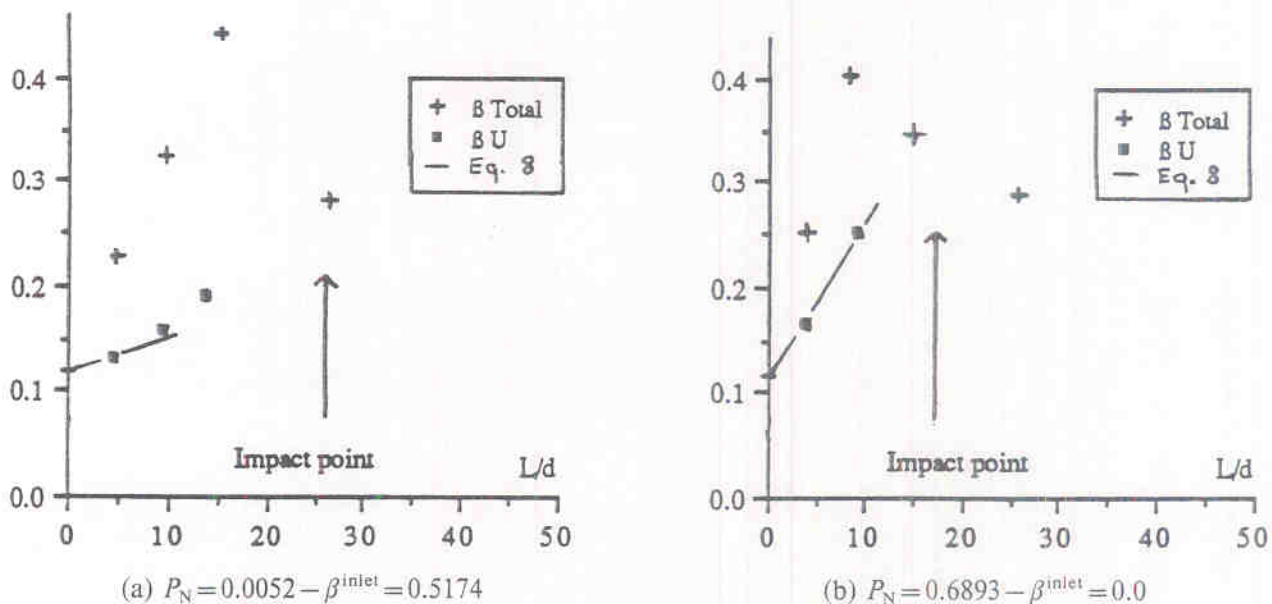(a) $P_N = 0.0052 - \beta^{inlet} = 0.5174$ (b) $P_N = 0.6893 - \beta^{inlet} = 0.0$

Fig. 6.   Dimensionless quantity of air entrained within the flow as a function of $L/d_0 - Fr = 13.55 - d_0 = 0.0315$ m [1].

Quantité adimensionnelle d'air entraînée au sein de l'écoulement en fonction de $L/d_0 - Fr = 13,55 - d_0 = 0,0315$ [1].

## 3.3   The fully-aerated flow region

From the lip of the aerator the non aerated core of the water jet is reduced along the channel while the flow is aerated through both the upper and lower free surfaces. For a jet subject to a low pressure gradient (i.e. $P_N < 0.1$) the experimental results of both Low [7] and the author indicate that the inner core of the jet becomes aerated at a distance $L_{C_{min}}$ from the end of the deflector such as (Fig. 1):

$$\frac{L_{C_{min}}}{d_0} = 10 \text{ to } 15 \tag{11}$$

and this result is independent of the Froude number. In presence of a large pressure gradient (i.e. $P_N > 0.5$) the author's results show that the distance $L_{C_{min}}$ decreases.

At the end of the deflector the rapid change of shear stress at the lower interface induces a high turbulence region. This suggests that a shear layer spreads from the lower interface across the jet (Fig. 1). From the junction of the entraining regions (i.e. $L = L_{C_{min}}$) to the position where the shear layer reaches the upper free surface (i.e. $L = L_{shear}$) there is a flow region with an aerated core and a turbulence gradient across the flow and it is suggested that air exchange may occur between the lower and upper flow regions but the mechanisms remain obscure.

For long jet lengths Low's [7] data show a marked change of the quantity of air entrained for $L/d_0 > 20$ (Fig. 7) and it is suggested that this position may correspond to the point where the growing shear layer reaches the upper free surface (Fig. 1). Low's data were obtained for low sub-pressures (i.e. $P_N < 0.1$) and the results are independent of the Froude number (Fig. 7):
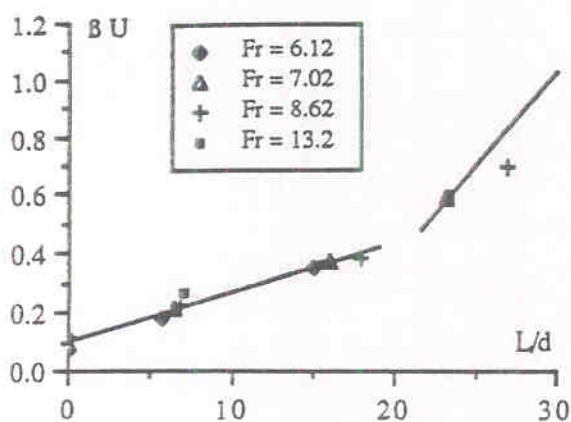
(a) Quantity of air entrained within the
    upper region

    Quantité d'air entraînée au sein
    de la zone supérieure
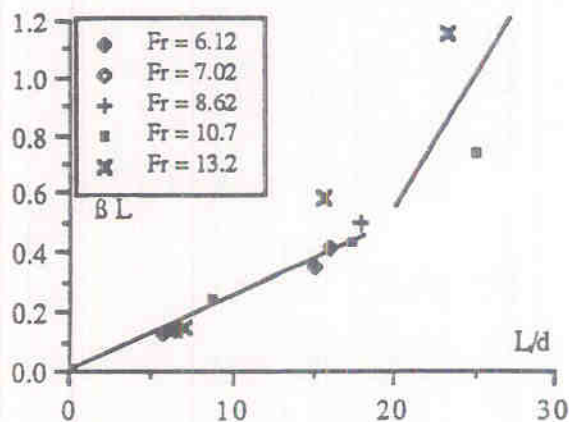
(b) Quantity of air entrained within the
    lower region

    Quantité d'air entraînée au sein
    de la zone inférieure

Fig. 7.   Quantity of air entrained within the upper and lower regions of the jet for $d_0 = 50$ mm – Low's data
          [7].

          Quantité d'air entraînée au sein des zones supérieure et inférieure du jet pour $d_0 = 50$ mm – résultats
          de Low [7].

$$\frac{L_{shear}}{d_0} = 20 \tag{12}$$

For $L > L_{shear}$ the Fig. 7 indicates an increase of the quantity of air entrained within the flow.

4   Conclusion

This paper presents a new approach of the aeration of free jet above a spillway. Two main parameters are the air demand of the aerator and the upper free surface aeration. For given flow conditions the air demand study provides the relationship $Q_{air}^{inlet} = f(\Delta P)$ and the operating point characterized by ΔP and Q_{air}^{inlet} is deduced for a given air duct geometry [7].
In the free surface aeration region simple considerations allow the estimation of the air concentration distribution and the air entrainment through the upper interface. The analytical solution provides a reasonable estimate of the upper air entrainment.
When the inner core of the flow becomes aerated greater knowledge of the air transfer between the lower and upper regions of the flow is required to estimate the air entrainment.

Notations

A_b bubble area in the direction perpendicular to the rise velocity (m²)

A_d duct area below the spillway surface (m²)

C air concentration defined as the volume of air per unit volume

C_d drag coefficient of a bubble

C_b air concentration near the spillway floor downstream of the aerator

C_{min} minimum air concentration in a section of a free jet

D diffusivity (m²/s)

d characteristic depth (m)

d_b air bubble diameter (m)

d_0 characteristic depth in the approach flow region (m)

F_b buoyant force (N)

Fr Froude number defined as: $Fr = \dfrac{V}{\sqrt{g * d}}$

g gravity constant (m/s²)

k_s equivalent uniform roughness (m)

L distance along the spillway from the end of the deflector (m)

$L_{c_{min}}$ distance from the end of the deflector where the inner core of the jet becomes aerated (m)

L_g groove length (m)

L_{jet} distance of the impact point from the end of the deflector (m)

L_{ramp} ramp length (m)

L_{shear} distance from the end of the deflector where the growing shear layer reaches the upper free surface of the jet (m)

P_{cavity} absolute pressure in the cavity beneath the nappe (Pa)

P_N pressure gradient number defined as: $P_N = \dfrac{\Delta P}{\varrho_w * g * d}$

P_0 absolute pressure above the flow (Pa)

Q_{air}^{inlet} air discharge provided by the air supply system (m³/s)

q_{air} quantity of air entrained within the flow per unit width (m³/s/m):

$$q_{air} = \int_0^{Y_{90}} C * V * dy$$

q_{air}^0 initial quantity of air entrained at the end of the deflector (m³/s/m)

q_{air}^{upper} net air entrainment through the upper free surface of the jet (m³/s/m)

Q_w water discharge (m³/s)

Re Reynolds number defined as: $Re = \dfrac{\varrho_w * V * d}{\mu}$

Tu turbulence intensity defined as: $Tu = \dfrac{u'}{V}$

t_s offset height (m)

U_w average water velocity (m/s) defined as: $U_w = \dfrac{q_w}{d}$

u' root mean square of axial component of turbulent intensity (m/s)

u_r rise bubble velocity (m/s)

V	velocity (m/s)
V_{90}	characteristic velocity at Y_{90} (m/s)
v_b	bubble volume (m^3)
W	channel width (m)
We	Weber number
x	direction along the spillway surface (m)
y	direction perpendicular to the spillway surface (m)
$Y_{C_{min}}$	characteristic depth where the air concentration is minimum $C = C_{min}$
Y_{10}	characteristic depth (m) where the air concentration is 10%
Y_{90}	characteristic depth (m) where the air concentration is 90%
α	spillway slope
β	dimensionless air discharge: $\beta = \dfrac{Q_{air}}{Q_w}$
β^L	dimensionless quantity of air entrained within the lower region of the jet in the aeration region ($Y_{90}^{lower} < y < Y_{C_{min}}$)
β^U	dimensionless quantity of air entrained within the upper region of the jet in the aeration region ($Y_{C_{min}} < y < Y_{90}^{upper}$)
ΔP	difference between the pressure above the flow and the air pressure beneath the nappe: $\Delta P = P_0 - P_{cavity}$
ϕ	angle between the ramp and the spillway
μ	dynamic viscosity of water (N·s/m^2)
ψ	lateral spread angle computed between Y_{90} and Y_{10}: $\tan \psi = \dfrac{Y_{90} - Y_{10}}{L}$
ψ^U	lateral spread angle at the upper free surface
ψ^L	lateral spread angle at the lower free surface
ϱ_{air}	density of air (kg/m^3)
ϱ_w	density of water (kg/m^3)
σ	surface tension between air and water (N/m)
θ	the angle between the water jet and the horizontal

References / Bibliographie

1. CHANSON, H., Study of Air Entrainment and Aeration Devices on Spillway Model, Research Report 88-8, Univ. of Canterbury, New Zealand, Oct. 1988.
2. CHANSON, H., Study of Air Entrainment and Aeration Devices, J. of Hyd. Res., IAHR, Vol. 27, No. 3, 1989, pp. 301–319.
3. CHANSON, H., Flow Downstream of an Aerator, Aerator Spacing, J. of Hyd. Res., IAHR, Vol. 27, No. 4, 1989, pp. 519–536.
4. CHANSON, H., Study of Air Demand on Spillway Aerator, J. of Fluids Eng., Trans. of ASME, Vol. 112, Sept. 1990, pp. 343–350.
5. COMOLET, R., Vitesse d'Ascension limite d'une Bulle de Gaz isolée dans un liquide peu visqueux (The terminal Velocity of a gas bubble in a liquid of very low velocity), J. de Mécanique appliquée, Vol. 3, No. 2, 1979, pp. 145–171.
6. ERVINE, D. A. and FALVEY, H. T., Behaviour of Turbulent Water Jets in the Atmosphere and in Plunge Pools, Proc. Instn. Civ. Engrs., Part 2, 1987, 83, Mar., pp. 295–314.
7. LOW, H. S., Model Studies of Clyde Dam Spillway Aerators, Research Report Ref. 86-6, Univ. of Canterbury, New Zealand 1986.
8. PETERKA, A. J., The Effect of Entrained Air on Cavitation Pitting, Joint meeting paper, IAHR/ASCE, Minneapolis, USA, Aug. 1953.
9. RUSSELL, S. O. and SHEEHAN, G. J., Effect of Entrained Air on Cavitation Damage, Canadian J. of Civil Eng., Vol. 1, 1974.
10. SPIEGEL, M. R., Mathematical Handbook of Formulas and Tables, McGraw-Hill Inc., New York, USA, 1974.
11. TAN, T. P., Model Studies of Aerators on Spillway, Research Report Ref. 84-6, Univ. of Canterbury, New Zealand, 1984.
12. VISCHER, D., VOLKART, P. and SIEGENTHALER, A., Hydraulic Modelling of Air Slots on Open Chute Spillways, Int. Conf. on Hyd. Mod., BHRA Fluid Eng., Coventry, England, Sept. 1982.
13. WOOD, I. R., Air Water Flows, 21st Congress IAHR, Aug. 1985, Melbourne, Australia.

APPENDIX 1

Theoretical calculation of the air entrainment through the upper free surface

Consider a small control volume in the free surface aeration region. The continuity equation on air is:

$$\frac{D}{Dt} C = - \operatorname{div} \vec{q}_{air}$$

where q_{air} is the air flux: $\vec{q}_{air} = - D * \vec{\nabla} C + C * \vec{u}_r$, C is the air concentration, D the diffusivity, u_r the rise velocity and we assume the air density is constant. The author [2] showed that the solution of the continuity equation is a Gaussian distribution. At the upper free surface we get:

$$C = erf \left[\frac{y}{\left[\sqrt{2 * \frac{D}{U_w} * x * \left(1 + \frac{u_r}{U_w} * \cos \theta * \frac{y}{x} \right)} \right]} \right]$$

where the function erf is defined as [10]:

$$erf(u) = \frac{1}{\sqrt{2 * \pi}} * \int_{-\infty}^{u} e^{-t^2/2} * dt$$

We define the free surface of the jet as the iso-air concentration line $C = 90\%$. The net upper air entrainment across the upper air-water interface from the lip of the aerator to a distance L becomes:

$$q_{air}^{upper} = \int_0^L \left(D * \frac{dC}{dy} - C * u_r * \cos\theta \right)_{y=Y_{90}} dx$$

where θ is the angle between the water jet and the horizontal. At the upper free surface $(y = Y_{90})$ the term dC/dy and the diffusivity D are estimated from the lateral spread angle ψ computed between Y_{90} and Y_{10}:

$$\left(\frac{dC}{dy} \right)_{y=Y_{90}} = \frac{K_0}{Y_{90} - Y_{10}}$$

$$D = \frac{1}{2} * \frac{U_w * L * (\tan\theta)^2}{1.2817}$$

where

$$K_0 = \frac{1}{\sqrt{2 * \pi}} * e^{-1/2 * (1.2817)^2}$$

$$Y_{90} - Y_{10} = \tan\psi * L + (Y_{90} - Y_{10})_{L=0}$$

Assuming that the air concentration follows a symmetrical distribution at the end of the deflector an estimate of the initial quantity of air entrained is:

$$\beta^0 = \frac{q_{air}^0}{q_w} \simeq \frac{1}{2} * \left(\frac{Y_{90} - Y_{10}}{d} \right)_{L=0}$$

Assuming that u_r and ψ are constant and replacing D and dC/dy with the above expressions the dimensionless air entrainment through the upper free surface becomes:

$$\frac{q_{air}^{upper}}{q_w} = K_0 * \left(\frac{L}{d_0} - 2 * \beta^0 * \mathrm{LN}\left(1 + \frac{1}{2} * \frac{\tan\psi}{\beta^0} * \frac{L}{d_0} \right) \right) - 0.90 * \frac{L}{d_0} * \frac{u_r}{U_w} * \cos\theta$$

where $u_r < 0$ is a fall velocity and $q_{air}^{upper} > 0$ is air entrainment.

APPENDIX 2

Rise velocity of an ellipsoïdal air bubble submitted to a pressure gradient

Let consider an air bubble in a pressure field. The forces on the rising bubble are:
1. the drag force $1/2 * C_d * \varrho_w * u_r^2 * A_b$;
2. the weight force $\varrho_{air} * g * v_b$;
3. the buoyant force F_b.

The drag force counterbalances the resultant of the weight force and the buoyant force:

$$1/2 * C_d * \varrho_w * u_r^2 * A_b = F_b - \varrho_{air} * g * v_b$$

If the shape of the bubble is approximated to a flat ellipsoïd of revolution the buoyant force is: $F_b = dP/dz * v_b$ where z is the vertical direction and the rise velocity becomes:

$$u_r^2 = \frac{2 * g * v_b}{C_d * A_b} * \left| \frac{\dfrac{dP}{dz}}{\varrho_w * g} - \frac{\varrho_{air}}{\varrho_w} \right|$$

For an air bubble submitted to a hydrostatic pressure gradient and neglecting the weight force $(\varrho_{air} \ll \varrho_w)$ the above formulation becomes:

$$u_r^2 \text{(Hydrostatic)} = \frac{2 * g * v_b}{C_d * A_b}$$

As far as the fluid viscosity is neglected (i.e. $d_b > 1.5$ mm) Comolet [5] showed that the rise bubble velocity may estimated as:

$$u_r^2 \text{(Hydrostatic)} = \frac{2.14 * \sigma}{\varrho_w * d_b} + 0.52 * g * d_b$$

Considering a water jet above an aerator on steep spillway and assuming that the pressure gradient is linear over the complete jet thickness d the rise velocity may be rewritten in term of the pressure gradient number P_N as:

$$u_r^2 = u_r^2 \text{(Hydrostatic)} * \left| P_N * \cos \theta - \frac{\varrho_{air}}{\varrho_w} \right|$$

where θ is the angle between the water jet and the horizontal.